PROJECTED CHANGES IN CLIMATOLOGICAL FORCING FOR COASTAL EROSION IN NSW

A Project Undertaken for the NSW Department of Environment and Climate Change

by

Kathleen L. McInnes[1], Deborah J. Abbs[1], Siobhan P. O'Farrell[1], Ian Macadam[1], Julian O'Grady[1] and Roshanka Ranasinghe[2]

[1]CSIRO Marine and Atmospheric Research
[2]Department of Environment and Climate Change

August 2007

Enquiries should be addressed to:

Dr Kathleen L. McInnes
CSIRO Marine and Atmospheric Research

Distribution list

Chief of Division

Project Manager

Client

Authors

Other CSIRO Staff

National Library

CMAR Libraries

Important Notice

Use of this Report

The use of this Report is subject to the terms on which it was prepared by CSIRO. In particular, the Report may only be used for the following purposes.

- this Report may be copied for distribution within the Client's organisation;
- the information in this Report may be used by the entity for which it was prepared ("the Client"), or by the Client's contractors and agents, for the Client's internal business operations (but not licensing to third parties);
- extracts of the Report distributed for these purposes must clearly note that the extract is part of a larger Report prepared by CSIRO for the Client.

The Report must not be used as a means of endorsement without the prior written consent of CSIRO.

The name, trade mark or logo of CSIRO must not be used without the prior written consent of CSIRO.

ISBN: 978-1-921424-11-3

CONTENTS

EXECUTIVE SUMMARY

Introduction

Coastal erosion can occur due to several factors. Increases in mean sea level and the frequency and/or intensity of severe storm events can increase the rate of offshore sediment transfer while changes in wind direction and hence wave direction can change the longshore transport of sediments causing erosion along some parts of the shoreline. The aim of this study is to investigate how the variables responsible for coastal erosion may change as a result of climate change due to the enhanced greenhouse effect for 2030 and 2070 planning horizons. In particular we investigate changes to wind and wave climate, storm surges, and the regional variations in mean sea level rise. An important aspect of this study is the consideration of the uncertainty of climate model responses for the relevant model variables.

Background and Methodology

Two locations have been selected for this study. The first location is the Clyde River/Batemans Bay system on the NSW south coast, being an example of a drowned river valley. The second is the Wooli Wooli River system on the NSW north coast which is a barrier estuary. The coastal responses obtained for these two study areas are expected to characterise the potential climate change impacts for these two geographically diverse coastal systems.

The range of different climate model responses to greenhouse gas forcing, and the uncertainty this represents often leads to the consideration of a high, a mid-range and a low scenario of climate change in impact assessments. However, in the present study, where a number of climate variables are of interest, each of which may vary differently with respect to each other the challenge has been to identify a pair of climate models that give as broad a range of responses as possible.

A pattern scaling technique is used to explore the range of responses in wind speed between different climate models. Wind speed is selected since it drives a number of processes that influence the coast such as waves and storm surge. This approach is used to identify two distinctly different model responses to a given climate forcing. The two models are then analysed in greater detail to derive other climate parameters such as wind direction, wind extremes, severe storms and regional sea level rise and these are in turn used to infer changes to the wave climate and storm surge return periods.

Wind Speed Changes and Model Selection

Pattern scaling is applied to five climate models for which daily wind speeds are available. Two regional climate models, CCM2 and CCM3, were found to have distinctly different climate change responses in wind speed over the NSW coastline. The CCM2 model undergoes wind speed decrease while the CCM3 model undergoes wind speed increase. Both CCM2 and CCM3 models are forced with the A2 emission scenario, where the atmospheric carbon dioxide concentrations rise from their present level of about 370 ppm to about 880 ppm by 2100. Given the current growth rate of CO_2 concentration (about 2ppm/year over the last 10 years), the A2 scenario may be considered a sufficiently conservative future scenario that is appropriate to base risk averse planning decisions on. Therefore, these two models were chosen for further analysis.

Changes in Wave Height and Wave Direction

Storm waves have the potential to change the cross-shore erosion volumes while shoreline orientation is strongly linked to the dominant swell wave conditions. The wind speed changes calculated for the different time slices in the CCM2 and CCM3 model are used to estimate the

changes to the wave climate for the two regions. Wave rider buoy data at Batemans Bay and Byron Bay (close to Wooli) are used to establish current climate wave information for the two locations.

Empirical relationships are used to convert model winds to significant wave height and period. Winds close to the coast are used to generate a time series of storm waves while winds offshore in the direction from which swell waves are observed to most frequently originate are used to generate swell waves and the two time series are combined. This technique is found to reproduce the observed wave frequencies well. Changes in the frequency of storm waves are investigated in the two climate models at 2030 and 2070 at Batemans Bay and Wooli. Storm waves originate most frequently from the southeasterly and southerly directions. In the CCM2 model, the occurrence frequencies of storm waves from S-SE octants tend to decrease whereas in the CCM3 model these occurrence frequencies tend to increase (Table A1).

At both locations, the changes in the average height and period of storm waves (waves > 3 m) are noisy with increases and decreases occurring in both models for different directions and time slices. However, the CCM3 model predicts an increase in the maximum storm wave height and period from the southerly, easterly and southeasterly directions at both coastal locations in 2070.

Changes in swell waves from the SSE octant (waves with directions varying from 135 and 180°) were investigated in both models at both future times. At Wooli, the frequency of occurrence of swell waves is found to increase in both models at both future times. In 2070, both models show a clockwise shift in swell waves. The average wave height and period of the swell waves increases in the CCM3 model while the CCM2 model shows an increase at 2030 and a decrease at 2070. At Batemans Bay, the frequency of occurrence of swell waves from the SSE octant is found to decrease in both models at both future times. It is possible that the decrease relates to a higher frequency of winds from the westerly direction at this latitude since the mid-latitude westerlies strengthen and contract to the south. The average directional change in SSE waves differs between models and time periods.

Changes in Storm Surge

Storm surges are caused by the strong winds and falling atmospheric pressure associated with severe weather systems. At Coffs Harbour, close to Wooli, extreme sea level events were found to be most commonly associated with cut-off low pressure systems in the Tasman Sea while frontal troughs were the second most common weather system associated with elevated sea levels. At Batemans Bay, the same two classes of events were associated with elevated sea levels except that the frontal troughs were the most common and cut-off lows the second most common. All weather systems associated with elevated sea level events produced southerly to south-easterly winds along the relevant coastal region.

Storm surge return periods were evaluated from extreme sea level residual data at Wooli and Batemans Bay using the Generalised Pareto Distribution (GPD) and yielded 50 year return periods of 0.61±0.12 m and 0.66±0.13 m respectively. To investigate the possible changes to storm surge frequency with climate change, the change in frequency of storm waves from a southerly to southeasterly direction was used to modify the appropriate parameters of the GPD. For 2070 the 50 year return periods increased to 0.64±0.14 m and 0.68±0.14 m at Wooli and Batemans Bay respectively under the frequency changes from the CCM3 model, and decreased to 0.59±0.11 m and 0.65±0.12 m under the frequency changes from the CCM2 model.

Regional Sea Level Rise

Relative to the 1990 level, global average mean sea level is likely to increase by 0.18 to 0.59 m by 2095, with a possible additional contribution from a future rapid dynamical response of the ice sheets of 0.1 to 0.2 m. However, these increases in sea level will not occur uniformly across the globe with some regions experiencing higher sea level rise and others lower. Such variations are due to spatial variations in the thermal expansion of the ocean.

The CSIRO Mark 2 and Mark 3 GCMs, used to provide boundary conditions for the CCM2 and CCM3 regional climate model simulations respectively, both suggest that future sea level rise along the NSW coast will be slightly higher than the global average projections. This result is associated with a strong warming of the sea surface temperatures in the region and a strengthening of the East Australian Current.

Summary and Recommendations

Ranges of change in key wave parameters that should be taken into consideration in future studies aiming to determine the physical impacts on coasts due to climate change are given below for 2030 and 2070 planning horizons (Table A1). Note that the dominant swell wave direction refers to the S-SE octant (i.e. directional range encompassing 135^0 to 180^0 clockwise from the North). Changes to storm characteristics given in Table A1 also relate to storms from the S-SE octant. Approximately 85 % of all NSW storms occur from this direction. Storms were defined as wave events where the significant wave height (Hs) exceeded 3m for at least 1 hour. All values, apart from the local sea level rise are projected changes from present values. The sea level values are projected changes relative to 1990-1999 values.

Table A1: *Ranges of climate change driven changes in key wave parameters for Wooli and Batemans Bay for 2030 and 2070.*

Location	**Wooli**				**Batemans Bay**			
Planning timeframe	**2030**		**2070**		**2030**		**2070**	
Model	**CCM2**	**CCM3**	**CCM2**	**CCM3**	**CCM2**	**CCM3**	**CCM2**	**CCM3**
Changes to Swell waves from dominant direction (135° to 180° from North)								
Direction	+0.3°	-0.8°	+1.2°	+0.1°	-0.4°	0.3°	+0.1°	-0.5°
Average Hs	0%	+8%	-7%	+8%	0%	8%	-8%	+8%
Changes to Storms from S-SE direction (135° to 180° from North)								
frequency of occurrence	-8%	+13%	-20%	+48%	-6%	+28%	-23%	+41%
Hs max of storms	+3%	0%	-15%	+9%	+7%	+11%	-6%	+32%
Changes to 100 year storm surge (above Mean Sea Level)								
Surge height	-1%	+1%	-3%	+4%	-1%	+1%	-3%	+1%
Local sea level rise (SLR) above projected global average sea level rise								
Model	**Mark2**	**Mark3**	**Mark2**	**Mark3**	**Mark2**	**Mark3**	**Mark2**	**Mark3**
Variation	0	+8cm	0	+12cm	0	+4cm	0	+12cm

The range of the parameter values predicted by the two different models in each case reflects the inherent uncertainty in modelling complex physical processes at large spatial and temporal scales. Therefore, any future studies adopting the climate change driven potential changes to coastal forcing parameters presented here should ideally consider several parameter values that lie within the ranges of change presented herein for 2030 and 2070 planning horizons. It should also be noted that the precautionary principle generally adhered to in planning and design

requires any risk based analysis to include the worst case scenario associated with the planning timeframes under consideration.

All modelled wind information used to estimate wave characteristics were extracted over selected offshore fetches so that the waves generated would be incident on the two study areas. The output was then averaged over 9 grid points representing an area of 120km $\times$ 120km centred on the two specific locations. Thus, the climate change driven changes to wave characteristics presented here for Wooli and Batemans Bay would also be directly applicable to any location that lies within a radius of at least 60km from the two locations.

With regard to sea level rise, the most recent projections of global average sea level rise (SPM, 2007) range from 18cm to 59cm by 2090-2100 relative to 1980-1999 levels. SPM (2007) further advises that the upper ranges of projected sea level rise could increase by 0.1-0.2m due to an additional contribution from a future rapid dynamical response of the ice sheets. Therefore, it is recommended that the ranges of local sea level rise (relative to the global average) given above be used in conjunction with a range of global average sea level rise of 18cm to 79cm by 2090-2100 relative to 1980-1999 levels.

Since the projections for the two locations, which are located on the far north and south coasts of NSW respectively, do not significantly differ from each other, it is likely that similar ranges of changes of swell and storm wave parameters may be applicable to coastal locations that lie in between Wooli and Batemans Bay. Pending more detailed information, the ranges of change for such intermediate locations could be reasonably inferred from the results presented herein.

1. INTRODUCTION

Communities and assets along the New South Wales coastline will increasingly come under threat from a range of climate change impacts. These include coastal flooding and erosion due to rising mean sea levels and possible changes in weather patterns that drive sea level extremes such as storm surges. In addition, estuaries along the NSW coast, may also suffer from increased flooding during extreme events and lower overall flows leading to water supply and quality issues.

Coastal erosion can occur due to several factors. Increases in mean sea level and the frequency and/or intensity of severe storm events can increase the rate of offshore sediment transfer while changes in wind direction and hence wave direction can change the longshore transport of sediments causing erosion along some parts of the shoreline. The aim of this study is to investigate how the environmental phenomena responsible for coastal erosion may change as a result of climate change. In particular we investigate possible changes to wind and wave climate, severe storms and storm surges, and the regional variations in mean sea level rise. An important aspect of this study is the consideration of the uncertainty of climate model responses for the relevant phenomena.

2. BACKGROUND AND METHODOLOGY

The range of different climate model responses to greenhouse gas forcing, and the uncertainty this represents, often leads to the consideration of a high, a mid-range and a low scenario of climate change in impact assessments. Often a high climate change scenario is associated with a ‘more severe’, or ‘worst case’ situation while a low scenario is associated with a ‘less severe’ or ‘best case’ scenario. This line of thinking maybe compromised when the change in the variable of interest is found to both increase and decrease under climate change conditions, depending on the model considered, so that the range of possible change spans zero. Such opposing responses can occur in different models forced by the same greenhouse gas emission scenario. This is an artefact of the differences in formulation of the models and their treatments of physical processes.

The concept of a high, mid and low scenario is further complicated when the impact of changes to several variables or different aspects of the same variable are being considered. For example, increases in wind speed may result in more severe storms, high waves and subsequent coastal erosion, which is a negative impact, yet decreases in wind speed may cause reduced mixing in estuaries which has an adverse effect on estuarine health. Furthermore, changes in wind direction cannot be classed in terms of a high and low response since a particular wind direction change may have a positive or negative impact at different points along a beach.

A final point concerns the issue of compatibility when considering changes to more than one variable. Is it physically realistic to combine particular changes in one variable with those of another or is the combination physically implausible?

These issues have been considered in formulating the approach adopted in the present study. We use a projection methodology commonly used by CSIRO (see Whetton et al., 2005), referred to hereafter as pattern scaling, to explore the range of responses among different climate models. We apply this approach to wind speed, a climate variable that drives a number of processes that influence the coast. This approach is used to identify two distinctly different model responses to a given climate forcing. The two models are then analysed in greater detail to derive other climate parameters such as wind direction, wind extremes, severe storms and regional sea level rise and these are in turn used to infer changes to the wave climate and storm surge return periods.

Two locations have been selected for this study. The first location is the Clyde River/Batemans Bay system on the NSW south coast, being an example of a drowned river valley. The second is the Wooli Wooli River system on the NSW north coast which is a barrier estuary. The coastal responses obtained for these two study areas are expected to characterise the potential climate change impacts for these two geographically diverse coastal systems.

Five climate models were selected for analysis in this study on the basis that model variables, including 10 m winds, were available on a daily time scale. The international models that CSIRO has analysed in previous studies (e.g. Hennessy et al., 2004) contain only monthly average fields of model variables.

The main details of the five models considered in this study are described briefly. The Mark 2 AOGCM is a nine-level atmospheric model coupled to a twelve-layer ocean model (Hirst et al., 2000). Several simulations of the Mark 2 model using different emission scenarios are available as detailed in Table 1. The CSIRO Mark 3 AOGCM has 18 vertical levels in the atmosphere and 31 levels in the ocean (Gordon et al. 2002). The DARLAM model is a regional atmospheric model which was run over Australia with 125 km horizontal resolution and nine vertical levels in the vertical. The lateral boundary conditions were taken from the Mark 2 GCM forced with the IS92a emission scenario. The Cubic Conformal Atmospheric Model (CCAM) is a stretched grid model in which the earth is mapped onto a cube (McGregor and Dix, 2001; McGregor, 2005). The resolution over Australia is approximately 60 km. In the low resolution regions of the model, the model solution is weighted heavily towards the solution of a GCM of uniform resolution. Two cubic conformal model simulations were considered in this study, the CCM2 simulation was nudged towards the results of the CSIRO Mark 2 GCM forced by the A2 emission scenario and the CCM3 simulation was nudged towards those of the CSIRO Mark 3 GCM also forced by the A2 emission scenario. Considering the current growth rate of CO_2 concentration of about 2ppm/year (over the last 10 years), the A2 scenario, where the atmospheric carbon dioxide concentrations rise from their present level of about 370 ppm to about 880 ppm by 2100, can be considered a sufficiently conservative future scenario that is appropriate to base risk averse planning decisions on.

Table 1: *Climate model simulations analysed in this report. Note that DARLAM, CCMk2 and CCMk3 are Regional Climate Models.*

Model	Emissions Scenarios post-1990 (historical forcing prior to 1990)	Horizontal resolution (km)
Mark2	IS92a, SRES A2 (four simulations), SRES B2	~400
DARLAM	IS92a	125
Mark3	SRES A2	~200
CCM2	Mark 2 SRES A2	~60
CCM3	Mark 3 SRES A2	~60

3. WIND SPEED CHANGES AND MODEL SELECTION

In this section a pair of models is selected whose changes to wind speed represent the upper and lower extremes of possible change over the region of interest. These models will then be analysed further to identify the associated changes to other variables of interest so that a plausible set of scenarios can be identified.

3.1 Pattern Scaling

Different models simulations may be forced with different emission scenarios and so to compare the climate change responses of different models or simulations of the same model with different climate change forcing, we apply the pattern scaling methodology of Whetton et al., (2005). In this approach, the time series of the variable of interest at each model grid point is linearly regressed against the model's globally averaged temperature time series to yield a map of variable change per degree of global warming. The patterns of change from different models can be directly compared with each other to identify the models with high and low climate

responses to greenhouse gas forcing. Note that in the event that several simulations with different emission scenarios have been performed with the same model, it has been the practice in past studies to average the response patterns since inspection reveals that they are similar, a result which is to be expected if the assumption of a linear relationship between temperature change and variable response is valid.

Figure 1 illustrates the lowest and highest ranked response from the five models (left). Examination of the individual model responses reveals that at the low end, it is mainly the CCM2 model that contributes to this pattern of wind speed decline while at the high end, it is the CCM3 model that exhibits the strongest wind speed increase with global warming. We therefore select these two models for further analysis.

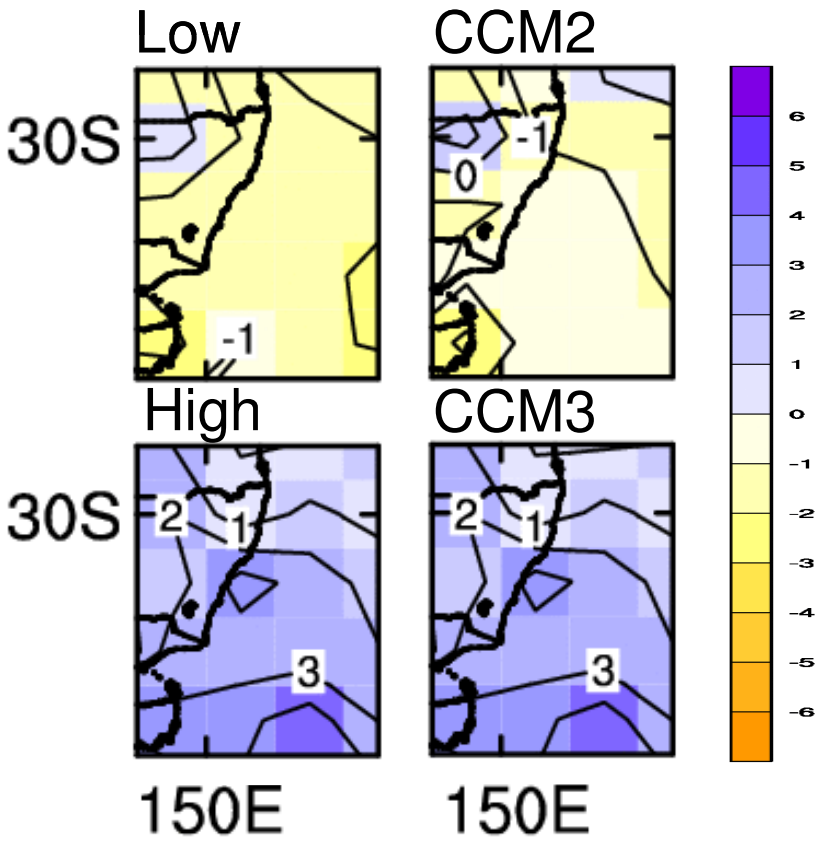

Figure 1: The lowest and highest response for annual average 10m wind speeds from the five models listed in table 1 (left) and the responses from the two CCAM simulations showing that CCM2 has a low climate change response and CCM3 has a high climate change response to the greenhouse gas forcing. Units are percentage change in wind per degree of global warming.

3.2 Comparison with Observations

Wind direction changes were analysed over the coastal regions of Batemans Bay (150-155°E, 34-39°S) and Wooli (153-158°E, 29-33°S). The modelled winds at grid points located within these windows were extracted over 40-year time slices centred on 1980, 2030 and 2070. These results were compared with equivalently processed data from the National Center for Environmental Prediction (NCEP) (Kalnay et al., 1996) reanalysis data set. The NCEP data set was created by running a weather forecast model in hindcast mode incorporating all available observations to produce a best estimate of the condition of the atmosphere at regular temporal and spatial intervals. It therefore serves as a verification data set in data sparse regions such as the oceans. NCEP winds were also extracted over the 40-year observational period to enable comparison of modelled winds. The winds were binned into eight directional and five speed classes to develop frequency matrices. The matrices were then averaged across all grid points

within an analysis window and the final results displayed as a wind rose. We note that due to the low resolution of the NCEP reanalyses available in this study (wind data available every 1.875° latitude and longitude), some features of the observed wind field that occur due to high resolution processes (e.g. channelling of wind by topography or gradients in the wind field due to sharp contrasts in terrain attributes such as friction) may not be adequately resolved.

The results for Batemans Bay and Wooli are shown in Figures 2 and 3 respectively and indicate some systematic differences between modelled winds and the NCEP reanalyses. For example, the CCM2 model produces a higher frequency of winds from the west, southwest and north in summer, autumn and spring which influences the annual average results. The CCM3 model produces a higher frequency of northerly winds in all seasons compared to the reanalyses. Both models show greater agreement with the observations during winter. To avoid model biases affecting the subsequent impact studies, we focus on the modelled *changes* between the different time slices, assuming that the changes are robust even though the climatology of the model may differ from the observed climatology. Furthermore, we focus on the changes to the winds that have an onshore component to the NSW coast, i.e. that range from 10° to 190°. These directions will be hereafter referred to as the 'oceanic' directions.

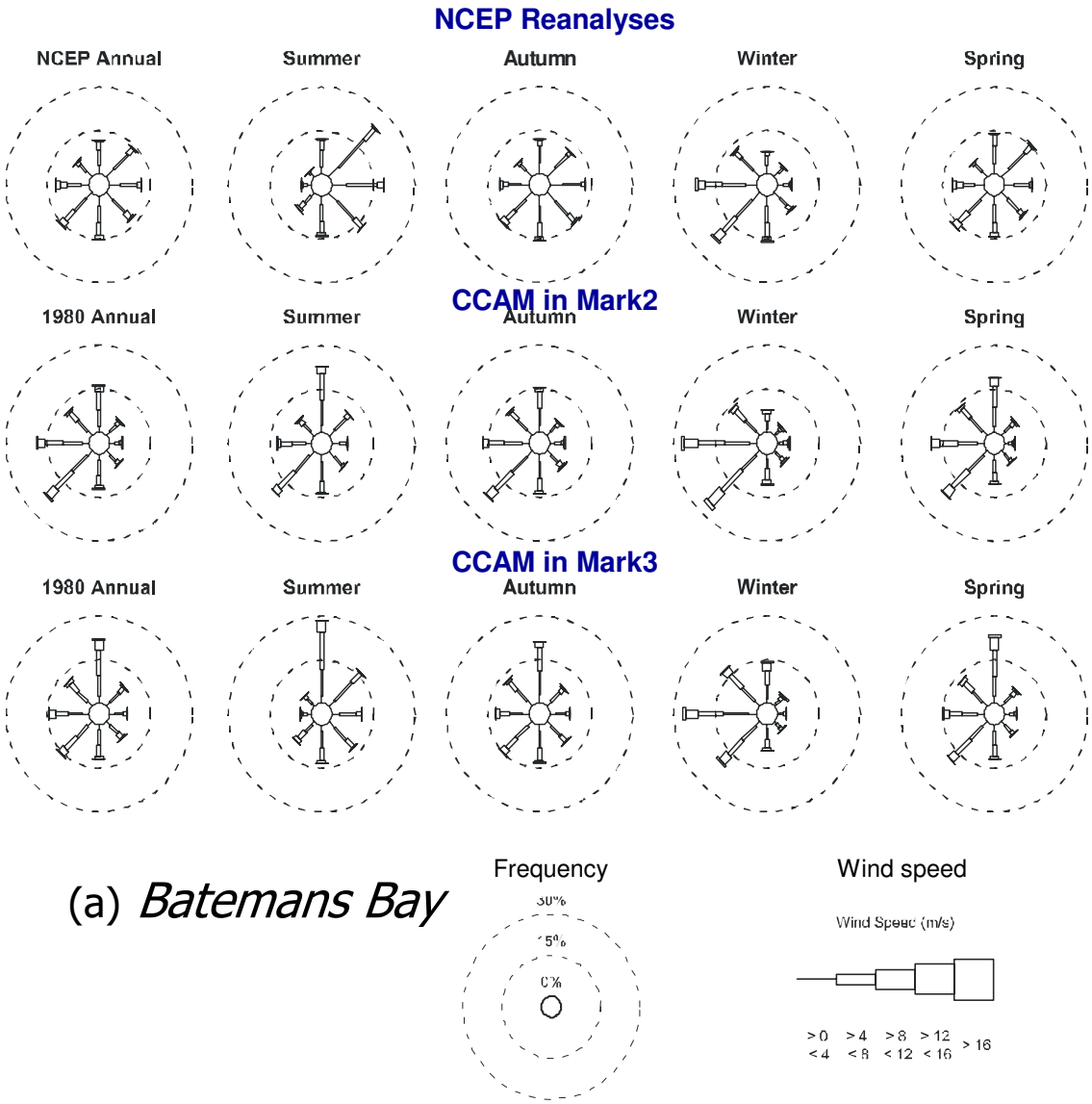

Figure 2: *Annual and seasonal wind roses for the 40 years from 1961 to 2000 derived from the NCEP reanalysis and the CCAM model nested in Mark 2 and Mark 3 respectively for the Batemans Bay region. Units are percent.*

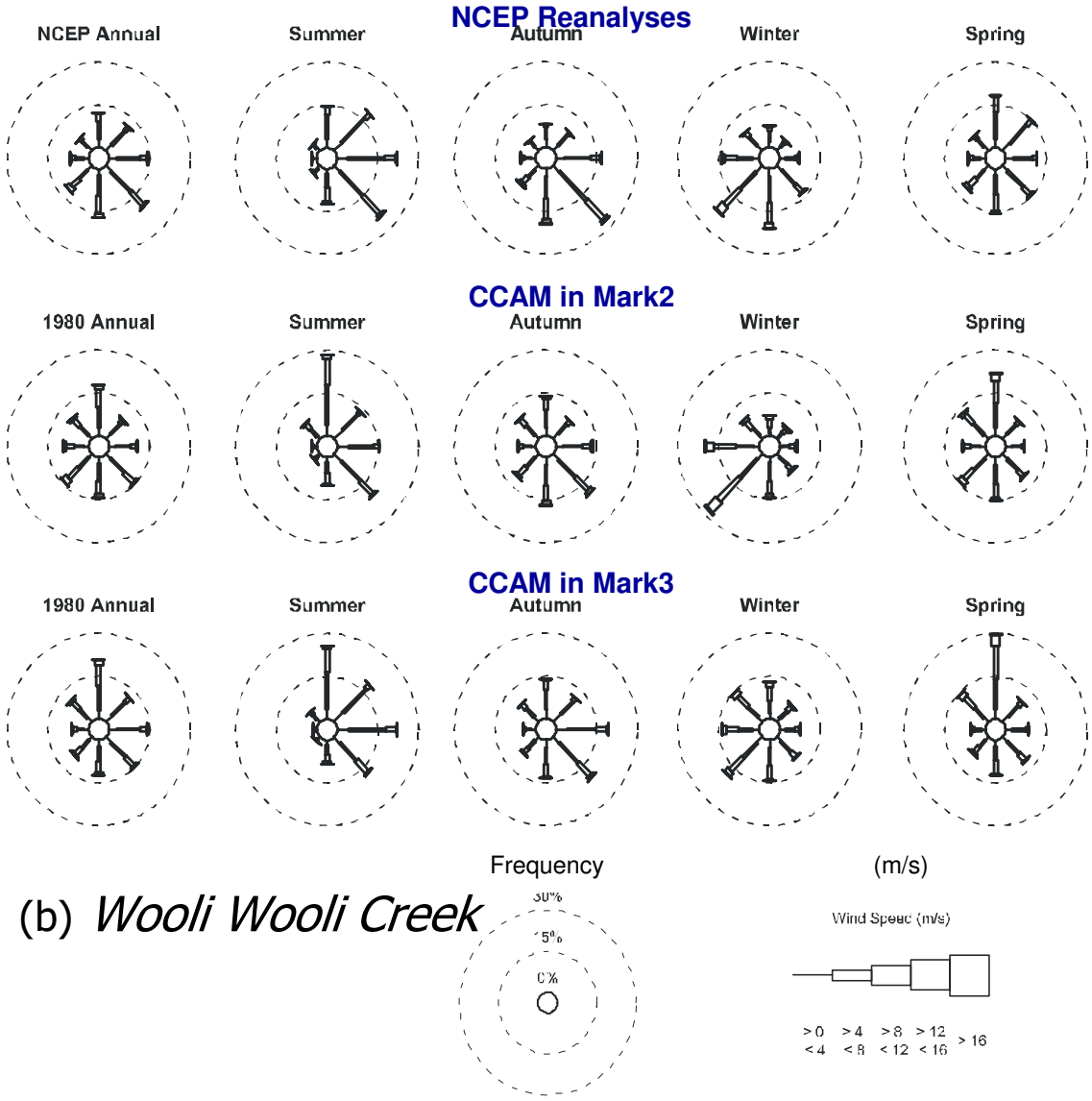

Figure 3: *Annual and seasonal wind roses for the 40 years from 1961 to 2000 derived from the NCEP reanalysis and the CCAM model nested in Mark 2 and Mark 3 respectively for Wooli Wooli. Units are percent.*

4. CHANGES IN WIND AND WAVE DIRECTION

The wind speed changes calculated for the different time slices in the CCM2 and CCM3 model are used to estimate the changes to the wave climate for the two regions. Wave rider buoy data at Batemans Bay and Byron Bay (close to Wooli) are used to establish current climate wave information for the two locations.

4.1 Methodology

A method for estimating waves from wind data in the climate models is developed for the purpose of estimating how waves may change in the future at Batemans Bay and Wooli due to changes in the wind climate. The wave climate at a particular location, is generated by local waves and swell. The latter is generated at remote locations and propagates, largely unattenuated over the deep ocean to the location of interest. Wave models forced by spatially and temporally varying wind fields represent the interaction of local and remotely generated

waves, but the use of such models is beyond the scope of the present study. Therefore a simpler yet robust method to deduce the wave changes from modelled wind data was derived using empirical equations commonly used in engineering applications for determining significant wave height and period for a given fetch under the assumption of a fully developed sea (Goda, 2003).

For locally generated waves, a time series of winds were developed from each of the two models at locations situated at the edge of the continental shelf close to the location of the wave rider buoys at Batemans Bay (151.0°E, 36.5°S) and Wooli (154.0°E, 31.0°S) respectively (approximately 100 km offshore). The winds from the 40-year time slices centred on 1980, 2030 and 2070 from the nearest model grid point and the surrounding eight grid points (constituting a 120kmx120km box) were averaged to produce a time series. The winds occurring from oceanic directions (10° to 190° from north) were converted to a significant wave height $H_{1/3}$ and wave period $T_{1/3}$ using the empirical relationships represented in (1) and (2) assuming a fully arisen sea (Goda, 2003) where g is the acceleration due to gravity, U is the wind speed measured 10 m above the sea surface and F is the fetch length assumed in this case to be 200 km;

$$gH_{1/3}/U^2 = 0.30\{1-[1+0.004(gF/U^2)^{1/2}]^{-2} \quad (1)$$

$$gT_{1/3}/(2\pi U) = 1.37\{1-[1+0.008(gF/U^2)^{1/2}]^{-5} \quad (2)$$

The wave directional climate derived from a 40 year time series centred on 1980 of model simulated winds with a directional component that is onshore to the coast (i.e. directions that range from 10° to 190°) at Byron Bay and Batemans Bay is illustrated in Figure 4.

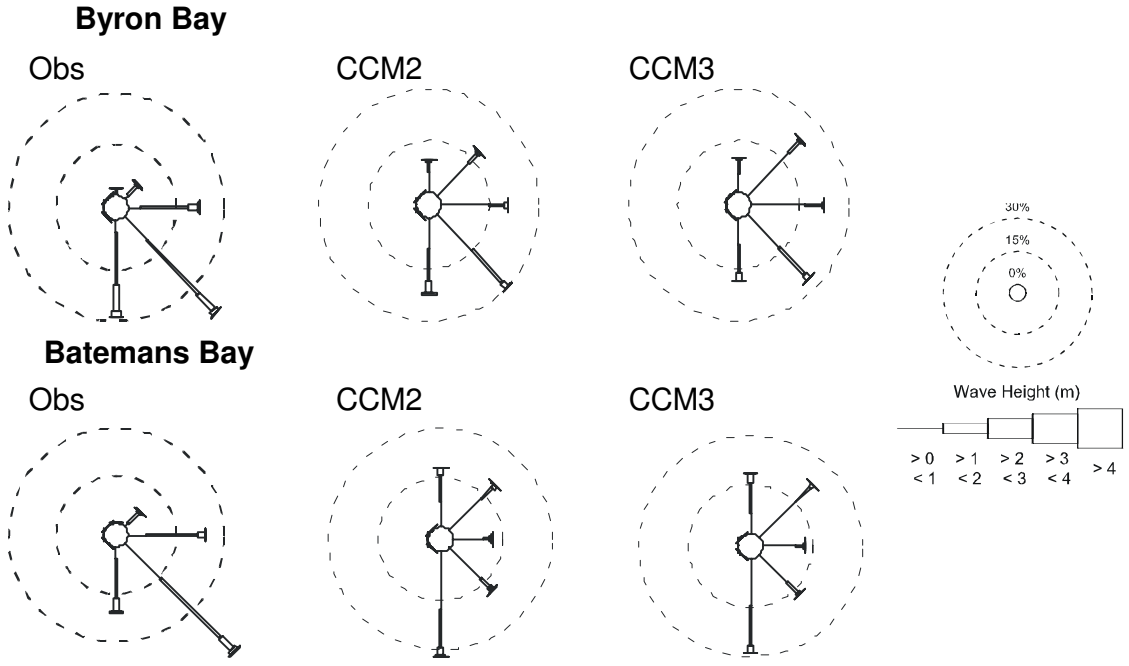

Figure 4: *The annual wave rose for 4 years of directional wave data from 1999 from the Byron Bay wave rider buoy and 5 years from 2001 of the Batemans Bay wave rider buoy and those derived from 40 years of model wind data centred on 1980 located at a maximum of 200 km offshore from the CCM2 and CCM3 model. Units are percent.*

Also shown are the wave directional roses derived from 4 years of directional Byron Bay data available from 1999 and 5 years of directional Batemans Bay data available from 2001. Note that although the time slices of the observations and the model data are of different and non-overlapping periods, it is not expected to significantly influence the analysis since the purpose here is to obtain the most realistic representation of waves from the modelled winds. Comparing the observed waves with the waves inferred from the modelled winds shows that the waves inferred from modelled winds from the northerly and northeasterly octants are over-represented

compared to winds from the southerly and southeasterly octants. A reason for this lack of agreement is likely to be due to the fact that the waves at a given location are made up in part of locally generated wind waves and remotely generated swell.

To represent the contribution due to swell waves, a radius of 500 km was drawn from each coastal location in the direction from which the majority of swell waves originate (155° and 151° clockwise from north for Byron Bay and Batemans Bay respectively). The locations of the 'swell' grid points were situated approximately in the central Tasman Sea, along a major storm track for mid-latitude cyclones which generate swell (Short and Trenaman; 1992). These winds were also converted to waves using (1) and (2) and a fetch length of 500 km in a similar manner to the local wind values. The 'swell wave' time series for each location and each model was then merged with the associated nearshore wave time series on the basis that if waves occurred from both sources on the same day, the attributes of the larger value of wave height were retained.

The wave roses derived using this approach, are compared with those from wave data for Byron Bay and Batemans Bay (Figure 5). These show that there is greater agreement between observations and model derived wave climates especially at Batemans Bay suggesting that the swell forms a significant component of the local wave climatology at this location. Furthermore, the improved agreement suggests that the approach is suitable for deriving information about future wave climate changes from climate models. The main deficiencies are that the models over-represent waves from the northerly octants and slightly underestimate waves from a southeasterly direction.

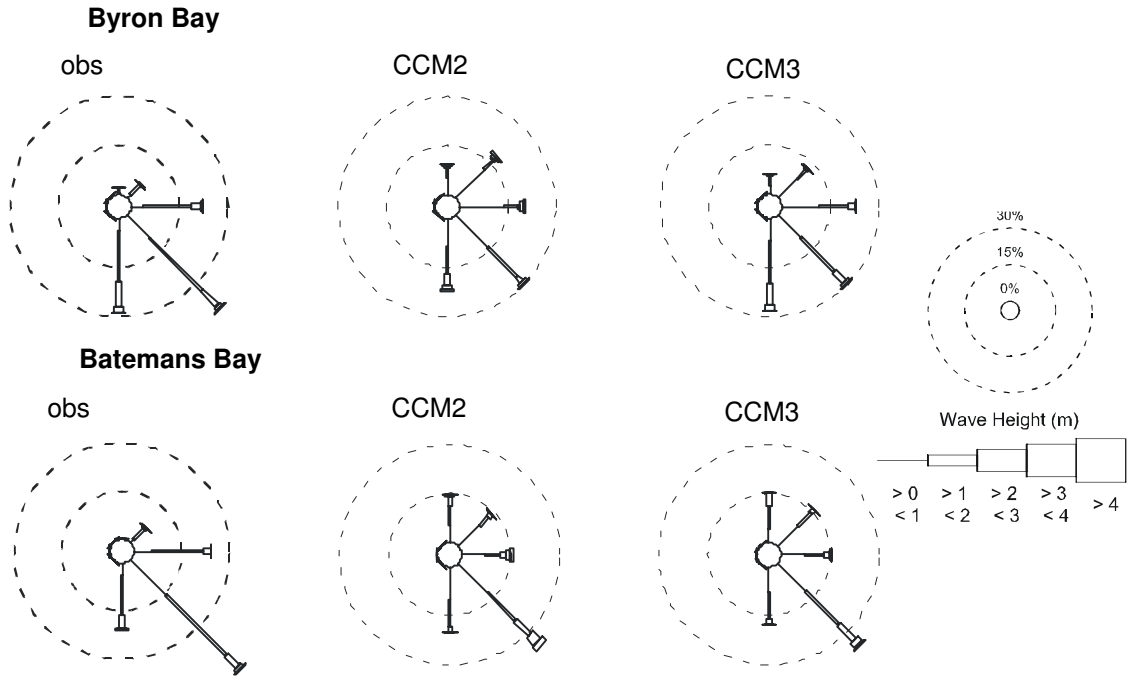

Figure 5: *The annual wave rose for 4 years of directional wave data from the Byron Bay wave rider buoy and 5 years of the Batemans Bay wave rider buoy and wave data derived from 40 years of model winds centred on 1980 located at a point approximately 200 km offshore in the CCM2 and CCM3 model combined with wind data located at around 500 km offshore in the direction from which the majority of swell waves arrive (the dominant swell wave direction). Units are percent.*

Also of interest in this study are 'storm waves' which, based on Lord and Kulmar (2000) are defined as wave events where the significant wave heights (H_s) exceeded 3 m for at least 1 hour. A comparison between observed and model derived storm waves for the two locations is shown in Figure 6 indicating a good agreement. However, the models over-represent waves from the northerly octants and slightly underestimate waves from a southeasterly direction.

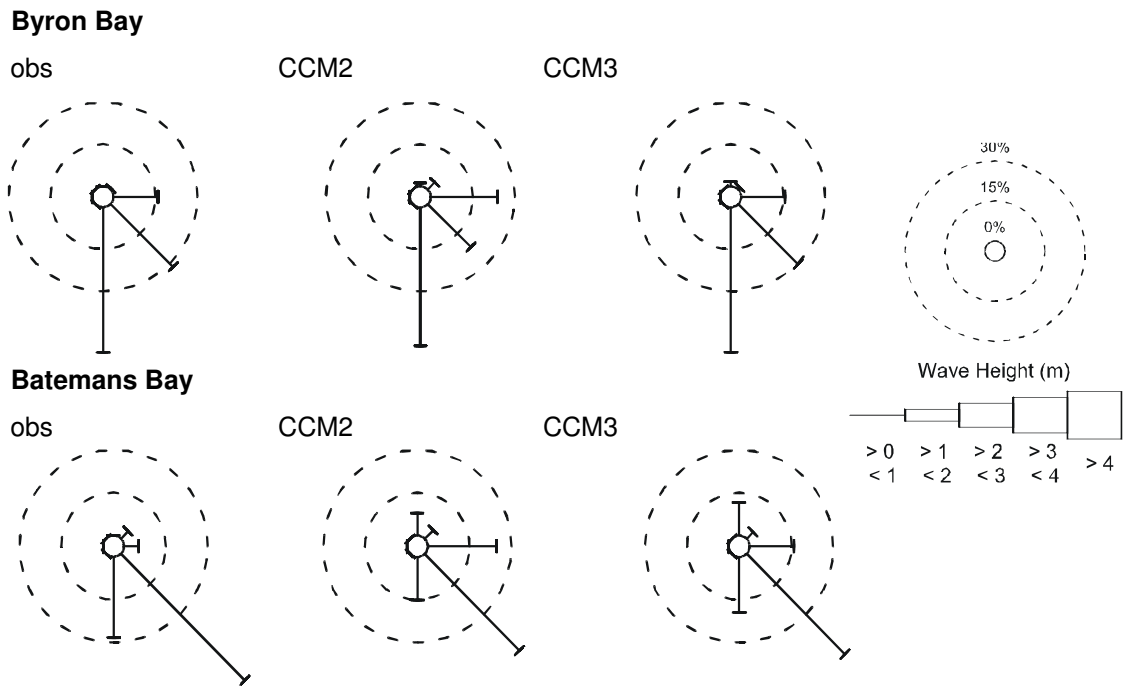

Figure 6: *As for Figures 4 and 5 but for storm waves (> 3m) derived from the Byron Bay and Batemans Bay wave rider buoy and wave data derived from model winds located at a maximum of 200 km offshore from the CCM2 and CCM3 model combined with wind data located at around 500 km offshore in the direction from which the majority of swell waves arrive from (the dominant swell wave direction). Units are percent*

4.2 Changes in Storm Waves

Changes in storm waves have the potential to change the cross-shore beach erosion volumes. To investigate the possible future changes to the shoreline due to this process we examine the changes in the storm waves (defined as wave events where the significant wave height (Hs) exceeded 3m for at least 1 hour) derived from the modelled winds in the time slices centred on 1980, 2030 and 2070. Table 2 presents the observed occurrence frequency of storm wave events per year and the changes to these occurrence frequencies in the future based on the two climate models at Wooli for the oceanic directions. Note that each directional bin in Tables 2 to 7 (i.e, NE, E, SE and S) span a directional range of 45° centred on the mean direction (i.e octants). For example the S octant ranges from 157.5° to 202.5° clockwise from North. The values of various parameters given for each directional bin are therefore averaged within the directional bin.

Table 2: *Observed occurrence frequency of storm events for Wooli. Units are number of events per year. The change in the occurrence frequency of waves in 2030 and 2070 compared with the 1980 model values. Decreases are shown in blue while changes greater than zero are shown in red. Units are percent.*

	CCM2					CCM3				
	NE	E	SE	S	S-SE combined	NE	E	SE	S	S-SE combined
obs	0.6	3.1	7.9	9.6	17.5	0.6	3.1	7.9	9.6	17.5
2030	-40.0	-49.5	-35.6	3.9	-8	100.0	2.7	-23.6	34.1	13
2070	-73.3	-54.5	-34.4	-13.7	-20	0.0	35.1	50.0	46.3	48

Tables 3 and 4 present the directional distribution of average Hs and Ts of storm waves over the three time periods in the model for Wooli. The changes tend to be noisy with little consistency

between time slice and direction. For example, the CCM2 model shows an increase in the average storm wave height and period from the dominant wave directions (SE and S) in 2030 and a decrease in 2070. CCM3 on the other hand shows a slight decrease of these values at both future times. However, the minimum storm wave height either remained unchanged or increased slightly at both time periods and all directions in both models except for the northeasterly direction in the CCM2 model. The maximum storm wave height increased across all directional categories in the CCM3 model by 2070 while the CCM2 model showed a decrease in the maximum height of waves from the SE and S directions and an increase from the NE and E categories at the same future time.

Table 3: *Wooli (a) average, (b) minimum and (c) maximum storm wave height (defined as waves > 3 m) estimated from the CCM2 and CCM3 climate models. Also shown are the changes between 2030 and 1980 and 2070 and 1980 coloured in blue for those less than zero and red for those greater than zero. Units are in metres.*

(a) Mean Hs

	CCM2					CCM3				
	NE	E	SE	S	S-SE combined	NE	E	SE	S	S-SE combined
1980	3.3	4.0	3.8	3.7	3.7	3.0	3.7	3.6	3.6	3.6
2030	3.3	3.9	4.1	3.8	3.9	3.2	3.8	3.5	3.6	3.5
	-0.1	-0.1	0.3	0.1	0.2	0.2	0.1	-0.1	-0.1	-0.1
2070	3.6	4.1	3.7	3.6	3.6	3.4	3.7	3.5	3.6	3.5
	0.2	0.1	-0.1	-0.1	-0.1	0.4	0.0	0.0	-0.1	-0.1

(b) Min Hs

	CCM2					CCM3				
	NE	E	SE	S	S-SE combined	NE	E	SE	S	S-SE combined
1980	3.1	3.0	3.0	3.0	3.0	3.0	3.0	3.0	3.0	3.0
2030	3.0	3.0	3.0	3.0	3.0	3.1	3.0	3.0	3.0	3.0
	-0.1	0.0	0.0	0.0	0.0	0.0	0.0	0.0	0.0	0.0
2070	3.1	3.0	3.0	3.0	3.0	3.3	3.0	3.0	3.0	3.0
	0.0	0.0	0.0	0.0	0.0	0.2	0.0	0.0	0.0	0.0

(c) Max Hs

	CCM2					CCM3				
	NE	E	SE	S	S-SE combined	NE	E	SE	S	S-SE combined
1980	3.8	7.0	6.9	6.6	6.7	3.1	5.0	5.0	5.4	5.3
2030	3.6	6.2	6.4	7.1	6.9	3.5	6.0	4.9	5.5	5.3
	-0.3	-0.9	-0.5	0.5	0.2	0.5	1.0	-0.1	0.1	0.0
2070	3.9	7.8	5.9	5.5	5.6	3.6	5.3	5.9	5.7	5.8
	0.1	0.8	-1.0	-1.1	-1.1	0.5	0.3	0.9	0.3	0.5

Table 4: *Wooli (a) average, (b) minimum and (c) maximum storm wave period (estimated from waves > 3 m) estimated from the CCM2 and CCM3 climate models. Also shown are the changes between 2030 and 1980 and 2070 and 1980 coloured in blue for those less than zero and red for those greater than zero. Units are in seconds.*

(a) Mean Ts

	CCM2					CCM3				
	NE	E	SE	S	S-SE combined	NE	E	SE	S	S-SE combined
1980	7.0	8.1	7.9	7.8	7.8	6.8	7.8	7.7	7.7	7.7
2030	7.0	8.0	8.2	7.8	7.9	7.0	7.9	7.6	7.7	7.6
	-0.1	-0.1	0.3	0.0	0.1	0.2	0.1	-0.1	-0.1	-0.1
2070	7.2	8.1	7.8	7.7	7.7	7.1	7.8	7.7	7.7	7.7
	0.2	0.1	-0.1	-0.1	-0.1	0.3	0.0	0.0	-0.1	0.0

(b) Min Ts

	CCM2					CCM3				
	NE	E	SE	S	S-SE combined	NE	E	SE	S	S-SE combined
1980	6.8	6.8	6.8	6.8	6.8	6.8	7.1	6.8	6.8	6.8
2030	6.7	6.9	6.8	6.7	6.8	6.8	7.2	6.8	6.7	6.8
	0.0	0.2	0.0	0.0	0.0	0.0	0.1	0.0	0.0	0.0
2070	6.8	6.8	6.8	6.8	6.8	7.0	6.9	6.9	6.8	6.8
	0.0	0.0	0.0	0.0	0.0	0.2	-0.2	0.1	0.0	0.0

(c)Max Ts

	CCM2					CCM3				
	NE	E	SE	S	S-SE combined	NE	E	SE	S	S-SE combined
1980	7.5	10.3	10.3	10.1	10.1	6.8	9.0	9.0	9.3	9.2
2030	7.2	9.8	9.9	10.4	10.3	7.2	9.7	8.9	9.3	9.2
	-0.2	-0.6	-0.3	0.4	0.2	0.4	0.7	-0.1	0.1	0.0
2070	7.6	10.8	9.6	9.4	9.4	7.2	9.2	9.6	9.5	9.5
	0.1	0.5	-0.6	-0.7	-0.7	0.5	0.2	0.7	0.2	0.3

At Batemans Bay also, there is a tendency for the CCM3 model to indicate an increase in the occurrence frequency of storm waves and for the CCM2 model to indicate a decrease in occurrence frequency (Table 5). The changes in the average height and period of storm waves are again noisy with increases and decreases occurring in both models for different directions and time slices (Tables 6 and 7). However, again, the maximum value of storm wave height and period in the CCM3 model tends to undergo a general increase in value.

Table 5: *Observed occurrence frequency of storm events at Batemans Bay. Units are number of events per year. Change in the occurrence frequency of waves in 2030 and 2070 compared with the 1980 model values. Decreases are shown in blue while changes greater than or equal to zero are shown in red. Units are percent.*

	CCM2					CCM3				
	NE	E	SE	S	S-SE combined	NE	E	SE	S	S-SE combined
obs	0.5	2	5.7	7.9	13.6	0.5	2	5.7	7.9	13.6
2030	6.7	-37.2	-17.3	28.3	-6	100.0	2.7	-23.6	34.1	28
2070	-60.0	-47.7	-28.6	-5.7	-23	0.0	35.1	50.0	46.3	41

Table 6: *Batemans Bay (a) average, (b) minimum and (c) maximum storm wave height (defined as waves > 3 m) estimated from the CCM2 and CCM3 climate models. Also shown are the changes between 2030 and 1980 and 2070 and 1980 coloured in blue for those less than zero and red for those greater than or equal to zero. Units are in metres.*

(a) Mean Hs

	CCM2					CCM3				
	NE	E	SE	S	S-SE combined	NE	E	SE	S	S-SE combined
1980	3.6	4.0	3.8	3.7	3.8	3.3	3.8	3.6	3.6	3.6
2030	3.0	3.0	3.0	3.0	3.0	3.4	3.4	3.5	3.6	3.6
	-0.5	-0.9	-0.8	-0.7	-0.8	0.0	-0.4	-0.1	0.0	0.0
2070	3.5	4.0	3.8	3.7	3.8	3.2	3.7	3.8	3.7	3.7
	0.0	0.1	-0.1	0.0	0.0	-0.1	-0.2	0.2	0.0	0.1

(b) Min Hs

	CCM2					CCM3				
	NE	E	SE	S	S-SE combined	NE	E	SE	S	S-SE combined
1980	3.0	3.0	3.0	3.0	3.0	3.0	3.0	3.0	3.0	3.0
2030	3.4	4.1	3.9	3.7	3.8	3.1	3.0	3.0	3.0	3.0
	0.4	1.1	0.9	0.7	0.8	0.1	0.0	0.0	0.0	0.0
2070	3.0	3.0	3.0	3.0	3.0	3.0	3.0	3.0	3.0	3.0
	0.0	0.0	0.0	0.0	0.0	0.0	0.0	0.0	0.0	0.0

(c) Max Hs

	CCM2					CCM3				
	NE	E	SE	S	S-SE combined	NE	E	SE	S	S-SE combined
1980	5.0	6.6	6.9	5.8	6.7	4.1	5.3	5.4	5.0	5.3
2030	4.2	6.3	7.5	6.1	7.2	3.9	5.8	5.5	7.1	5.9
	-0.7	-0.3	0.6	0.3	0.5	-0.2	0.5	0.1	2.1	0.6
2070	4.8	6.7	6.2	6.5	6.3	3.9	5.9	6.9	7.2	7.0
	-0.2	0.1	-0.8	0.7	-0.4	-0.2	0.6	1.5	2.2	1.7

Table 7: *Batemans Bay (a) average, (b) minimum and (c) maximum storm wave period (estimated from waves > 3 m) estimated from the CCM2 and CCM3 climate models. Also shown are the changes between 2030 and 1980 and 2070 and 1980 coloured in blue for those less than zero and red for those greater than or equal to zero. Units are in seconds.*

(a) Mean Ts

	CCM2					CCM3				
	NE	E	SE	S	S-SE combined	NE	E	SE	S	S-SE combined
1980	7.2	7.9	7.9	7.7	7.9	7.0	7.9	7.8	7.7	7.7
2030	7.1	8.0	8.0	7.6	7.9	7.1	7.6	7.8	7.6	7.7
	-0.1	0.1	0.0	-0.1	0.0	0.0	-0.3	0.0	-0.1	0.0
2070	7.2	8.0	7.9	7.8	7.8	6.9	7.7	7.9	7.6	7.8
	0.0	0.1	0.0	0.0	-0.1	-0.1	-0.2	0.2	-0.1	0.1

(b) Min Ts

	CCM2					CCM3				
	NE	E	SE	S	S-SE combined	NE	E	SE	S	S-SE combined
1980	6.7	6.7	6.9	6.8	6.8	6.8	7.2	6.8	6.8	6.8
2030	6.8	6.8	6.7	6.7	6.7	6.8	6.8	6.9	6.8	6.8
	0.0	0.0	-0.1	0.0	-0.1	0.0	-0.5	0.1	-0.1	0.0
2070	6.7	6.8	6.8	6.8	6.8	6.7	6.8	6.8	6.7	6.8
	0.0	0.0	-0.1	0.0	0.0	0.0	-0.4	0.0	-0.1	0.0

(c) Max Ts

	CCM2					CCM3				
	NE	E	SE	S	S-SE combined	NE	E	SE	S	S-SE combined
1980	8.3	10.1	10.3	9.6	10.1	7.7	9.2	9.3	9.0	9.2
2030	7.8	9.9	10.6	9.8	10.4	7.5	9.6	9.3	10.4	9.6
	-0.5	-0.2	0.3	0.2	0.3	-0.2	0.4	0.0	1.4	0.4
2070	8.2	10.2	9.8	10.0	9.9	7.5	9.6	10.3	10.5	10.3
	-0.1	0.1	-0.5	0.4	0.2	-0.2	0.4	1.0	1.5	1.1

4.3 Changes in Swell Waves

Shoreline orientation is strongly linked to the dominant swell wave conditions. Possible changes to swell waves are investigated in the model derived waves at the future times compared with those obtained under current climate. Based on analysis of wave data from Byron Bay and Batemans Bay, the dominant swell wave directions are 155° and 151° clockwise from north respectively. Therefore for this analysis, the waves with a direction that lie between 135° and 180° from north (hereafter, the SSE octant) are averaged to produce a dominant wave direction and changes to this direction are estimated. We note that this will remove the influence of cyclone events which may occur to the north during the summer months. Other characteristics such as average significant wave height and wave period incident from the dominant SSE octant are also investigated. The results for Wooli and Batemans Bay are shown in Tables 8 to 11.

At Wooli, the occurrence frequency of swell waves from the SSE octant is found to increase by not more than 2 % in both models at both future times (Table 8). In 2070, both models show a clockwise shift in swell waves in the SSE octant. However at 2030 there is a less clear signal

with CCM2 showing a clockwise shift and CCM3 an anticlockwise shift for waves from the SSE Both models predict very small changes in average significant wave heights and wave periods at both future times.

At Batemans Bay, the occurrence frequency of swell waves from the SSE octant is found to decrease in both models at both future times by up to 2.1% (Table 9). It is possible that the decrease relates to a higher frequency of winds from the westerly direction at this latitude since the mid-latitude westerlies may strengthen and contract to the south. The average directional change in SSE waves is not consistent between models and time periods. The CCM2 model shows an anticlockwise shift in swell at 2030 (up to 0.4) but a clockwise shift in SSE swell of 0.12° in 2070 whereas the CCM3 model indicates a clockwise shift of 0.25° in SSE swell at 2030 and an anticlockwise shift of 0.47° in 2070. Both models predict very small changes in average significant wave heights and wave periods at both future times.

Table 8: *Changes to the characteristics of swell waves from the SSE (the directional range of 135° and 180°) at Wooli. Note that a positive direction change is a clockwise rotation.*

	CCM2				CCM3			
	Occurence frequency %	Average Direction	Average H sig	Average T sig	Occurrence Frequency	Average Direction	Average H sig	Average T sig
1980	25.3	159.4	1.4	4.6	26.0	159.4	1.2	4.5
2030	25.7	159.6	1.4	4.7	26.3	158.6	1.3	4.6
	0.4	0.3	0.0	0.1	0.3	-0.8	0.1	0.1
2070	25.3	160.6	1.3	4.5	28.0	159.4	1.4	4.7
	0.0	1.2	-0.1	-0.1	2.0	0.1	0.1	0.2

Table 9: *Changes to the characteristics of swell waves from the SSE (the directional range of* 135° and 180°) *at Batemans Bay. Note that a positive direction change is a clockwise rotation.*

	CCM2				CCM3			
	Occurrence frequency %	Average Direction	Average H sig	Average T sig	Occurrence Frequency	Average Direction	Average H sig	Average T sig
1980	32.7	159.1	1.3	4.6	27.8	158.0	1.3	4.7
2030	31.2	158.6	1.3	4.7	27.4	158.3	1.4	4.8
	-1.5	-0.4	0.0	0.0	-0.4	0.3	0.1	0.1
2070	30.6	159.2	1.3	4.6	26.8	157.5	1.4	4.9
	-2.1	0.1	0.0	-0.1	-0.9	-0.5	0.1	0.2

For waves from all oceanic directions (10° to 190° clockwise from North), the average wave direction is generally predicted to shift anti-clockwise by not more than 3.3° at Wooli (Table 10) for both future times. While the changes predicted by both models to H_s and T_s at both future times are very small, the CCM2 model predicts a decrease of both H_s and T_s in 2070 (of the order of 0.1), whereas the CCM3 model predicts an increase of the same order for both parameters at the same future time.

At Batemans Bay when waves from all oceanic directions are considered, the average wave direction is predicted to shift anti-clockwise by not more than 2.1° by 2030, while it is predicted to shift clockwise by not more than 3.8° by 2070 (Table 11). The inconsistent changes predicted by both models to H_s and T_s at both future times are very small (of the order of 0.1).

Table 10: *Changes to the characteristics of swell waves within the directional range of* 10^0 and 190° *at Wooli. Note that a positive direction change is a clockwise rotation.*

	CCM2			CCM3		
	Average Direction	Average H sig	Average T sig	Average Direction	Average H sig	Average T sig
1980	109.2	1.3	4.5	100.7	1.2	4.5
2030	106.1	1.2	4.5	101.3	1.2	4.6
	-3.1	0.0	0.0	0.6	0.0	0.1
2070	105.9	1.2	4.4	99.4	1.3	4.6
	-3.3	-0.1	-0.1	-1.3	0.1	0.1

Table 11: *Changes to the characteristics of swell waves within the directional range of* 10^0 and 190° *at Batemans Bay. Note that a positive direction change is a clockwise rotation.*

	CCM2			CCM3		
	Average Direction	Average H sig	Average T sig	Average Direction	Average H sig	Average T sig
1980	98.5	1.5	4.8	95.8	1.4	4.7
2030	96.4	1.5	4.8	94.8	1.4	4.7
	-2.1	0.0	0.0	-1.0	0.0	0.0
2070	97.2	1.4	4.7	98.6	1.4	4.8
	0.8	-0.1	-0.1	3.8	0.0	0.1

5. CHANGES IN STORM SURGE

Storm surges are caused by the strong winds and falling atmospheric pressure associated with severe weather systems. In this section we use tide gauge records to evaluate storm surge return periods. A synoptic typing technique is applied to the sea level pressure patterns on the days in which storm surge events occurred to illustrate the types of storm systems responsible for storm surge. Finally we use the estimated frequency changes to storm waves to estimate the possible changes in return periods of storm surges under future climate conditions.

5.1 Storm Surges

Hourly sea level residual data (sea level data with the astronomical tides removed) were obtained for 10 tide gauges along the NSW coast for the purpose of evaluating return periods for storm surges. Data from a tide gauge at Batemans Bay was available for the period 1989-2005, although only the data for 1989-2001 were considered owing to some suspect data in the post-2001 period. Datasets from two tide gauges within the Wooli Wooli estuary (at the entrance and at the caravan park) revealed short periods of highly elevated water levels associated with heavy rainfall and so were deemed unsuitable for an analysis of storm surge heights. Instead, tide gauge data from Coffs Harbour, which was highly correlated with the Wooli Wooli entrance data, were used as a basis for analysing storm surge heights at Wooli Wooli entrance (The correlation coefficient between the Wooli Wooli entrance and Coffs Harbour time series was 0.84). Coffs Harbour data was available for the period 1996-2005. From each tide gauge, a time series of daily maximum sea level residuals was generated.

Short data gaps in the Batemans Bay and Coffs Harbour time series were filled using appropriately scaled data from alternative gauges whose time series were highly correlated with

the time series of interest. Batemans Bay data gaps were filled with scaled Port Kembla data. The correlation coefficient between the Batemans Bay and Port Kembla time series was 0.59. Coffs Harbour data were filled with scaled Port Stephens data. The correlation coefficient between the Coffs Harbour and Port Stephens time series was 0.77. This method of filling gaps in the Batemans Bay and Coffs Harbour time series was deemed to be adequate for the purposes of identifying extreme storm surge heights. The generation of complete time series for other types of analysis may merit a more sophisticated treatment of data gaps.

A sample of extreme storm surge events was identified from each time series using a threshold approach such that an event was defined as occurring while the residuals exceeded a threshold μ m. The maximum residual attained during the event was extracted. For each time series, a value of μ was selected to yield a sample of peak storm surge heights suitable for analysis using extreme value statistics. A μ value of 0.22 m was selected for the Batemans Bay time series, yielding 168 events over a 13 year period. A value of 0.20 m was selected for Coffs Harbour, yielding 137 events over a 10 year period. It was possible to augment the small Coffs Harbour sample and generate a 30 year sample of 384 events by adding 23 peak storm surge heights of 0.32 m or greater reported by MHL (1991) for the period 1971-1990. The smaller events in the 30 year sample were represented by repeating the peak storm surge heights less than 0.32 m in the original 10 year sample three times (this assumes that the behaviour of smaller events in the 1971-1990 period is similar to that of those for the 1996-2005 period). A linear relationship, based on a comparison of time series of daily maximum sea level residuals, was then used to transform the Coffs Harbour data, R_{CH}, to levels typical for Wooli, R_{WW}:

$$R_{WW} = 0.906R_{CH} + 0.015 \quad (3)$$

The Generalized Pareto Distribution (GPD), which has the advantage of making use of all available extreme value data (Coles, 2001), was fitted to each of the samples. For each sample the fitted GPD was then used to obtain a return period curve for peak storm surge heights (Figure 7) and to estimate peak heights for extreme storm surges occurring with return periods longer than the period represented by the sample (Table 12). Although estimates of 100 year return levels are given for Batemans Bay, given the time period represented by the Batemans Bay sample, these estimates may be unreliable. The poor fit of the GPD to three of the four most extreme Wooli data may indicate that the fitted GPD does not adequately describe the distribution of a larger population of extreme data and hence that the return levels for very extreme events at Wooli are also unreliable. However, GPDs fitted to just the more extreme Wooli data yield physically unrealistic return period curves and it may be the case that the three events are more extreme than would be expected from a larger population of events and that the empirical return periods assigned to them in Figure 7 are too small. Investigation of these issues is ongoing and the return period curves in Figure 7 are presented only to provide an illustration of the impact of possible future changes in storm frequency on storm surge height return levels.

Table 12: *Current climate peak storm surge height return levels (m) for Batemans Bay and Wooli with 95% confidence intervals.*

Location	Return Period (years)			
	10	20	50	100
Wooli	0.48 ±0.06	0.53 ±0.08	0.61 ±0.12	0.67 ±0.16
Batemans Bay	0.57 ±0.08	0.61 ±0.10	0.66 ±0.13	0.70 ±0.16

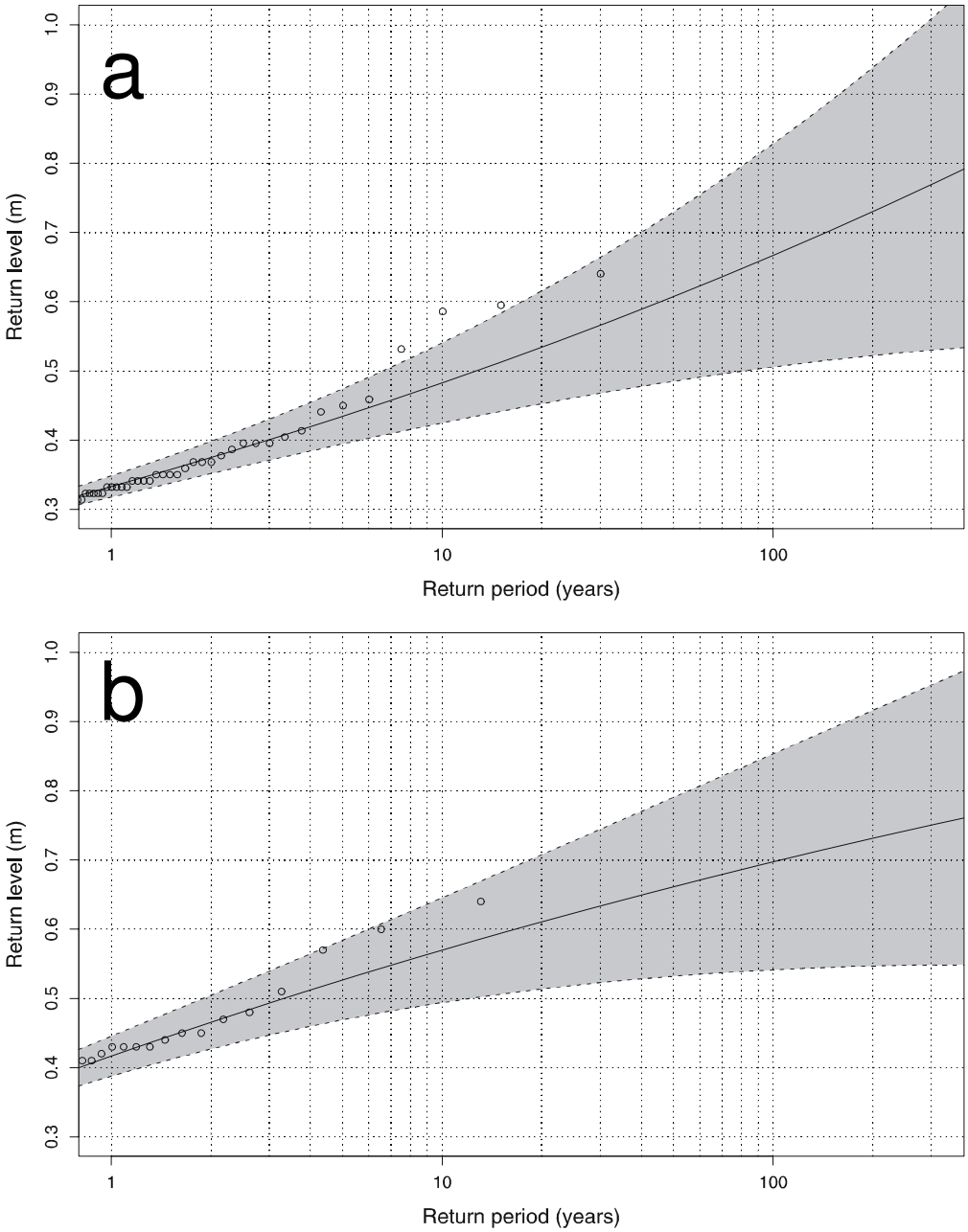

Figure 7: *Peak storm surge height return levels for (a) Wooli and (b) Batemans Bay. 95% confidence intervals for the return levels are shown in grey. Circles depict recorded peak storm surge heights.*

5.2 Weather Events Associated with Storm Surges

In this section, a brief examination of the weather systems and associated wind directions that are associated with storm surges is undertaken so that changes to storm surge occurrence may be inferred from the changes in wind and wave direction. A synoptic typing procedure that identifies similarities in daily analyses of sea level pressure is applied to the 40 year time slice of reanalysis data centred on 1980 and the equivalent time slice from the climate model simulations to investigate the meteorological systems responsible for storm surges at both locations.

The severe sea level residual events (those greater than 0.32 m for Coffs Harbour and 0.34 m for Batemans Bay) identified in the previous section were used as a basis for the synoptic typing. The Coffs Harbour events were selected over a 30 year period while Batemans Bay events were selected over a 13 year interval as described in the previous section. The mean sea level pressure patterns from the extreme sea level days were analysed using a synoptic typing technique in which fields are grouped using Pearson product-moment correlations (see Appendix 1 and Yarnal, 1993). Similar fields are identified on the basis of similar spatial structures (i.e. highs and lows in similar positions) with little emphasis on the magnitude of the patterns. The typing was carried out over the region bounded by 145° and 165°E and 25° and 45°S.

For the Coffs Harbour sea level residual data, the synoptic typing yielded four synoptic types which are illustrated in Figure 8. The first pattern (Figure 8a) is one of a cut-off low situated off the east coast of Australia producing south-easterly winds along the east coast. The second pattern (Figure 8b) resembles a frontal trough associated with a low pressure system in the southern ocean producing southerly winds along the east coast (cold front). The pattern presented in Figure 8c shows a Tasman Low bringing southerly winds to the east coast. The final pattern presented in Figure 8d resembles an ex-tropical cyclone with a ridge of high pressure to the south. The winds produced by this pattern are southeasterly on the northern NSW coast. A summary of the percentage of storm surge events that are caused by each type of system is presented in Table 13. Elevated sea level events at Batemans Bay consisted of two key synoptic patterns which were similar to those shown in Figures 8 a-b for Coffs Harbour. Cold fronts were associated with 58% of elevated sea level events while cut-off lows were associated with 22% of elevated sea level events.

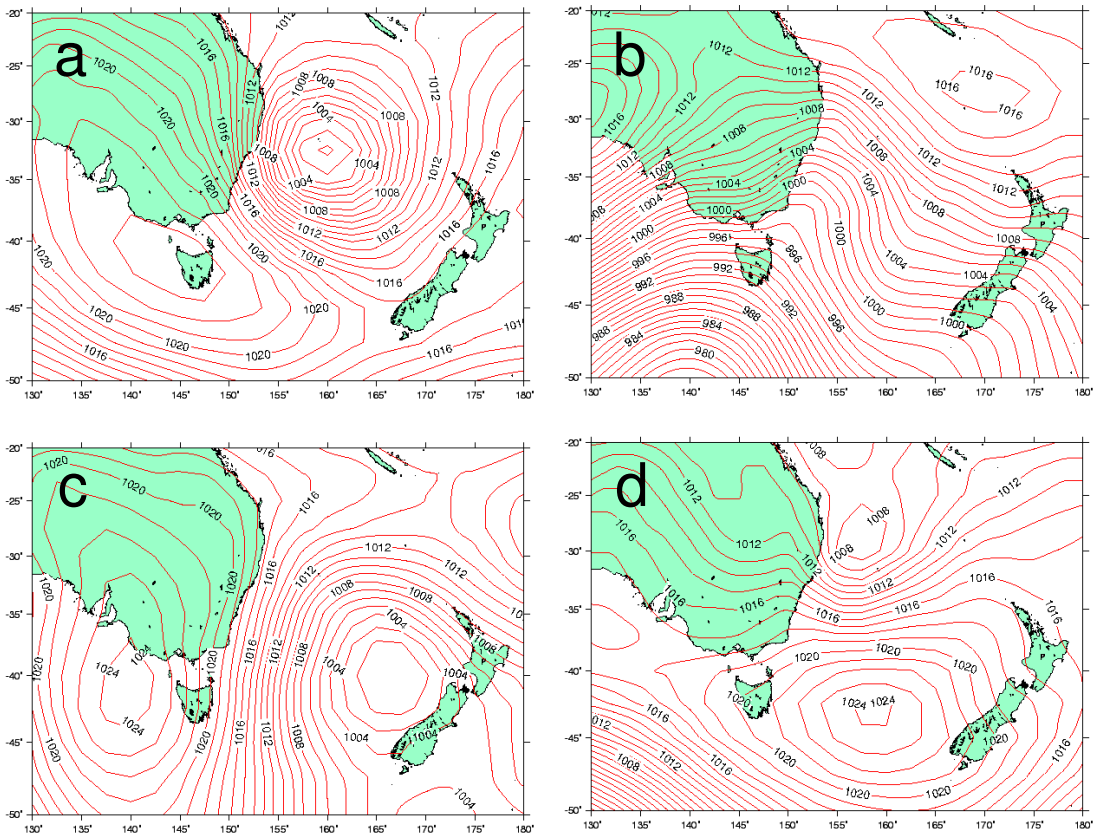

Figure 8: *The four key synoptic types associated with elevated sea level events (sea levels greater than 0.32 m) at Coffs Harbour.*

The key finding of this work is that the occurrence of extreme sea level events is associated with the occurrence of southeasterly to southerly winds. This suggests that the change in frequency of severe winds or waves from those directions can be used as a proxy to assess the changing frequency of storm surge events. .

Table 13: *Percentages of extreme sea level events at Coffs Harbour and Batemans Bay and the typical coastal wind direction associated with each synoptic type. Note that 7% of synoptic events at Coffs Harbour and 20% of events at Batemans Bay remained unclassified.*

Synoptic Type	Typical Wind Direction	Coffs Harbour	Batemans Bay
Cut-off low	South-easterly	42	22
Cold front	Southerly	21	58
Tasman low	Southerly	17	0
Ex-tropical cyclone	South-easterly (at Coffs Harbour)	13	0

5.3 The Impact of Climate Change on Storm Surges

The weather patterns associated with extreme sea level events were found to comprise low pressure systems in the Tasman or fronts for which the winds in the vicinity of the coast are mainly from the southeast or southerly directions. Therefore, we infer changes in the *occurrence* frequency of storm surge events under future climate conditions from the changes in frequency of the storm wave occurrences for waves from the SE and S octants. The changes in *occurrence* frequency of storm waves for 2030 and 2070 relative to 1980 are summarised in Table 14. From these we infer that storms decrease in frequency of occurrence in the CCM2 model while they increase in frequency of occurrence in the CCM3 model.

Table 14: *The number of storm wave events from the SE and S octants (combined) in the 1980 climate and changes in occurrence frequency (in percent) of storm waves from the SE and S octants (combined) in 2030 and 2070.*

Location	Year	CCM2	CCM3
Wooli	1980	295	195
	2030	-8%	+13%
	2070	-20%	+48%
Batemans Bay	1980	221	149
	2030	-6%	+28%
	2070	-23%	+41%

The changes in occurrence frequency are used to infer changes to the height of storm surges for given return periods. This is achieved by perturbing the average number of events per year *N* using (4) for each sample of extreme storm surge events according to the changes in the occurrence frequency of storm wave events, *Δf,* given in Table 14 and refitting the GPD.

$$N_{future} = N_{current}(\Delta f + 100)/100 \qquad (4)$$

Estimates of peak storm surge height return levels for 2030 and 2070 on the basis of the CCM2 and CCM3 models are given in Table 15. These show that the decreases in the *occurrence* frequencies of storms suggested by CCM2 are associated with slight decreases of the order of 1 to 2 cm in peak storm surge height return levels as the 21st Century progresses. The increases in the frequencies of storms suggested by CCM3 are associated with increasing peak surge height return levels of the order of 1 to 3 cm.

Table 15: *The peak storm surge height return levels (m) at Wooli and Batemans Bay, with 95% confidence intervals.*

Location	Model	Year	Return Period (years)			
			10	20	50	100
Wooli		1980	0.48 ± 0.06	0.53 ± 0.08	0.61 ± 0.12	0.67 ± 0.16
	CCM2	2030	0.48 ± 0.06	0.53 ± 0.08	0.60 ± 0.12	0.66 ± 0.16
		2070	0.47 ± 0.05	0.52 ± 0.07	0.59 ± 0.11	0.65 ± 0.15
	CCM3	2030	0.49 ± 0.06	0.54 ± 0.09	0.62 ± 0.13	0.68 ± 0.17
		2070	0.51 ± 0.07	0.56 ± 0.10	0.64 ± 0.14	0.70 ± 0.19
Batemans Bay		1980	0.57 ± 0.08	0.61 ± 0.10	0.66 ± 0.13	0.70 ± 0.16
	CCM2	2030	0.57 ± 0.07	0.61 ± 0.10	0.66 ± 0.13	0.69 ± 0.15
		2070	0.55 ± 0.07	0.60 ± 0.09	0.65 ± 0.12	0.68 ± 0.15
	CCM3	2030	0.58 ± 0.08	0.62 ± 0.11	0.67 ± 0.14	0.71 ± 0.17
		2070	0.59 ± 0.09	0.63 ± 0.11	0.68 ± 0.14	0.71 ± 0.17

6. REGIONAL SEA LEVEL RISE

Mean sea level rise occurs as a result of two main processes; a) the melting of land based ice, which increases the mass of the ocean and b) decreases in ocean density, which increase the volume of the ocean. Increases in ocean volume occur largely due to increases in the heat content of the ocean and so the density change component is often referred to as thermal expansion. The amount of thermal expansion varies spatially due to the influence of ocean currents and spatial variations in ocean warming.

Relative to the 1990 level, global average mean sea level is likely to increase by 0.18 to 0.59 m by 2095, with potentially an additional contribution from a future rapid dynamical response of the ice sheets of possibly 0.1 to 0.2 m (SPM, 2007). However, these increases in sea level will not occur uniformly across the globe with some regions experiencing higher levels of sea level rise and others lower. Such variations are due to variations in the thermal expansion of the ocean. Thermal expansion accounted for about half of the observed sea level rise over the period 1993 to 2006 and is expected to be the dominant contribution to sea level rise during the 21st century.

Here, we examine the relative sea level rise along the NSW coast due to thermal expansion in two CSIRO GCMs; the Mark 2 and the Mark 3 models. These two models provided the boundary conditions for the CCM2 and CCM3 regional climate model simulations respectively. Figure 9 shows the thermal expansion from these models for 2070 relative to 1990-1999 values In both models the thermal expansion is higher than global average values in this region and is largest for the Mark 3 model. This result is associated with the stronger warming of the sea surface temperatures in this region and a strengthening of the East Australian Current. These figures suggest that future sea level rise along the NSW coast will be slightly higher than the global average projections. These additional amounts are summarised in Table 16 for Batemans Bay and Wooli.

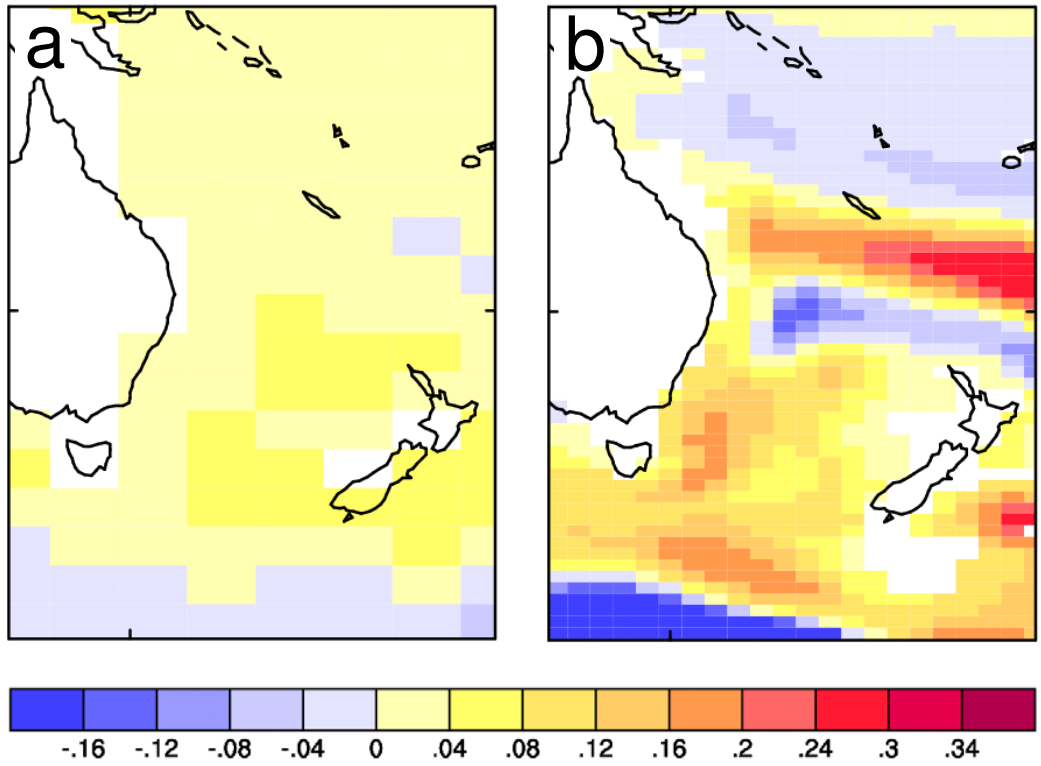

Figure 9: *The spatial pattern of thermal expansion relative to the global average thermal expansion in (a) the Mark 2 GCM and (b) the Mark 3 GCM for a ten year time slice centred on 2070 relative to 1990-1999 values.*

Table 16: *Increase in sea level rise due to thermal expansion along the NSW coast relative to the global average values.*

Location	Year	Low Mark 2 (m)	High Mark 3 (m)
Batemans Bay	2030	0-0.04	0-0.04
	2070	0-0.04	0.08-0.12
Wooli	2030	0-0.04	0.04-0.08
	2070	0-0.04	0.08-0.12

7. SUMMARY AND RECOMMENDATIONS

This study has investigated the possible changes to coastal forcing conditions due to climate change for 2030 and 2070 planning horizons. The study has highlighted the complexity of issues that surround defining a consistent set of scenarios from climate models that can demonstrate a marked range of responses to a particular climate forcing scenario. Coasts are influenced by, among other things, waves and storm surges, both of which are influenced by wind speed. This variable has therefore been used as the basis for selecting a pair of models that span the range of response to enhanced greenhouse gas forcing of the models considered in this study. The two selected models have been analysed in more detail with regards to changes in wave extremes and direction, inferred from the daily wind information over time slices centred on 1980, 2030 and 2070.

Ranges of change in key wave parameters relevant for future studies aiming to determine the physical impacts on coasts due to climate change are given below for 2030 and 2070 planning horizons (Table 17). Note that the dominant swell wave direction refers to the S-SE octant (i.e.

directional range encompassing 135° to 180° clockwise from the North). Changes to storm characteristics given in Table 17 also relate to storms from the S-SE octant. Approximately 85 % of all NSW storms occur from this direction. Storms were defined as wave events where the significant wave height (Hs) exceeded 3m for at least 1 hour.

Table 17: *Ranges of climate change driven changes in key wave parameters for Wooli and Batemans Bay for 2030 and 2070.*

Location	**Wooli**				**Batemans Bay**			
Planning timeframe	**2030**		**2070**		**2030**		**2070**	
Model	**CCM2**	**CCM3**	**CCM2**	**CCM3**	**CCM2**	**CCM3**	**CCM2**	**CCM3**
Changes to Swell waves from dominant direction (135° to 180° from North)								
Direction	+0.3°	-0.8°	+1.2°	+0.1°	-0.4°	0.3°	+0.1°	-0.5°
Average Hs	0%	+8%	-7%	+8%	0%	8%	-8%	+8%
Changes to Storms from S-SE direction (135° to 180° from North)								
frequency of occurrence	-8%	+13%	-20%	+48%	-6%	+28%	-23%	+41%
Hs max of storms	+3%	0%	-15%	+9%	+7%	+11%	-6%	+32%
Changes to 100 year storm surge (above Mean Sea Level)								
Surge height	-1%	+1%	-3%	+4%	-1%	+1%	-3%	+1%
Local sea level rise (SLR) above projected global average sea level rise								
Model	**Mark2**	**Mark3**	**Mark2**	**Mark3**	**Mark2**	**Mark3**	**Mark2**	**Mark3**
Variation	0	+8cm	0	+12cm	0	+4cm	0	+12cm

The range of the parameter values predicted by the two different models in each case reflects the inherent uncertainty in modelling complex physical processes at large spatial and temporal scales. Therefore, any future studies adopting the climate change driven potential changes to coastal forcing parameters presented here should ideally consider several parameter values that lie within the ranges of change presented herein for 2030 and 2070 planning horizons. It should also be noted that the precautionary principle generally adhered to in planning and design requires any risk based analysis to include the worst case scenario associated with the planning timeframes under consideration.

All modelled wind information used to estimate wave characteristics were extracted over selected offshore fetches so that the waves generated would be incident on the two study areas. The output was then averaged over 9 grid points representing an area of 120km × 120km centred on the two specific locations. Thus, the climate change driven changes to wave characteristics presented here for Wooli and Batemans Bay would also be directly applicable to any location that lies within a radius of at least 60km from the two locations.

With regard to sea level rise, the most recent projections of global average sea level rise (SPM, 2007) range from 18cm to 59cm by 2090-2100 relative to 1980-1999 levels. SPM (2007) further advises that the upper ranges of projected sea level rise could increase by 0.1-0.2m due to an additional contribution from a future rapid dynamical response of the ice sheets. Therefore, it is

recommended that the ranges of local sea level rise (relative to the global average) given above be used in conjunction with a range of global average sea level rise of 18cm to 79cm by 2090-2100 relative to 1980-1999 levels.

Since the projections for the two locations, which are located on the far north and south coasts of NSW respectively, do not significantly differ from each other, it is likely that similar ranges of changes of swell and storm wave parameters may be applicable to coastal locations that lie in between Wooli and Batemans Bay. Pending more detailed information, the ranges of change for such intermediate locations could be reasonably inferred from the results presented herein.

As a final precautionary comment, it should be noted that in this study, an attempt has been made to select a pair of models with markedly different responses to the same greenhouse forcing to establish an estimate of the range of possible change in future coastal forcing conditions. However, the pool of models from which this choice was made was limited by the need to also have daily model output for the subsequent more detailed analysis. Therefore it is possible that an even larger range of climate change response may have been identified if a larger number of models had been assessed.

ACKNOWLEDGMENTS

The work of the authors draws upon research findings of many colleagues within CSIRO Marine and Atmospheric Research and overseas research institutions. CSIRO global and regional climate models were developed by the members of the Climate, Weather and Ocean Prediction Theme of CSIRO Marine and Atmospheric Research.

Tide gauge and wave data were provided by the Manly Hydraulics Laboratory. Part of this work was funded by the Australian Greenhouse Office through the Australian Climate Change Science Program. The authors wish to acknowledge valuable comments by Dr Mark Hemer from CSIRO Marine and Atmospheric Research and Mr. David Hanslow and Mr. Doug Lord of the NSW Department of Environment and Climate Change.

REFERENCES

Coles, S.G., 2001: An Introduction to Statistical Modeling of Extreme Values. Springer.

Goda, Y., (2003) Revisiting Wilson's Formulas for simplified wind-wave Prediction. *J. Waterway, Port, Coastal and Ocean Eng.* Vol. 129, No. 2, 93-95.

Gordon, H.B., Rotstayn, L.D., McGregor, J.L., Dix, M.R., Kowalczyk, E. A. Waterman, L. J., Hirst, A. C., Wilson, S. G., Collier, M. A., Watterson, I. G. and Elliott, T. I. 2002: The CSIRO Mk3 climate system model. Technical paper 60. CSIRO Atmospheric Research 134 pp. http://www.cmar.csiro.au/e-print/open/gordon_2002a.pdf

Hennessy, K, K. McInnes, D. Abbs, R. Jones, J. Bathols, R. Suppiah, J. Ricketts, T. Rafter, D. Collins and D. Jones, 2004: Climate Change in New South Wales Part 2: Projected changes in climate extremes*. Report for the New South Wales regional Office. 79 pp.*

Hirst, A. C., O'Farrell, S. P., and Gordon, H. B. 2000: Comparison of a coupled ocean-atmosphere model with and without oceanic eddy-induced advection. Part I: Ocean spinup and control integrations. J. Climate, 13 (1): 139-163.

Kalnay, E., M. Kanamitsu, R. Kistler, W. Collins, D. Deaven, L. Gandin, M. Iredell, S. Saha, G. White, J. Woollen, Y. Zhu, A. Leetmaa, B. Reynolds, M. Chelliah, W. Ebisuzaki, W.Higgins, J. Janowiak, K. C. Mo, C. Ropelewski, J. Wang, R.Jenne, and D. Joseph, 1996: The NCEP/NCAR 40-Year Reanalysis Project. Bull. Amer. Meteor. Soc., 77, 437–471.

Lord, D., Kulmar, M., 2000. the 1974 storms revisited: 25 years experience in ocean wave measurement along the south-east Australian coastline. Proceedings, 27th International Conference on Coastal Engineering. ASCE, Sydney, pp. 559–572.

McGregor, J. L., and M. R. Dix, 2001: The CSIRO conformal-cubic atmospheric GCM. In IUTAM Symposium on Advances in Mathematical Modelling of Atmosphere and Ocean Dynamics, P. F. Hodnett (Ed.), Kluwer, Dordrecht, 197-202.

McGregor, J. L., 2005: C-CAM: Geometric aspects and dynamical formulation [electronic publication]. CSIRO Atmospheric Research Tech. Paper No. 70, 43 pp.

MHL 1991: Storm surges monitored along the New South Wales coast March – April 1990. Manly Hydraulics Lab Report 591, 23pp.

Short, A. D. and N. L. Trenaman, 1992: Wave climate of the Sydney region, an energetic and highly variable ocean wave regime Aust. J. Mar. Freshwater Res., 43, 765-791.

SPM 2007: Contribution of Working Group I to the Fourth Assessment Report of the Intergovernmental Panel on Climate Change. Summary for Policymakers. 18pp http://www.ipcc.ch/SPM2feb07.pdf

Whetton, P. H., K. L. McInnes, R. N. Jones, K. J. Hennessy, R. Suppiah, C. M. Page, J. Bathols, P. Durack (2005) Climate change projections for Australia for impact assessment and policy application: A review. CSIRO technical report. 33 pp. http://www.cmar.csiro.au/e-print/open/whettonph_2005a.pdf

Yarnal, B., 1993: Synoptic Climatology in Environmental Analysis: A Primer. Belhaven Press, London.

APPENDIX I– SYNOPTIC TYPING

The synoptic typing procedure follows the method of Yarnal (1993) and is a correlation based pattern-typing technique in which fields of gridded numerical data are grouped based on Pearson product-moment correlations. Similar fields are identified on the basis of similar spatial structures (i.e. highs and lows in similar positions) with little emphasis on the magnitude of the patterns.

To establish a synoptic climatology compatible with the output from the climate models, this technique was first applied to 00 UTC MSLP reanalysis fields valid for the extreme wind days. These fields spanned the region between 140 and 160°E and 35 and 45°S and contained 64 (6x6) gridpoints. The following steps were then applied to the data set.

Each MSLP field is normalised:

$$Z_i = \frac{x_i - \overline{X}}{s}$$

where Z_i is the normalised value at a grid-point i, x_i is the initial value at gridpoint i, $\overline{X}$ is the mean of $X_{i=1\ to\ N}$ where N is the number of grid points and s is the standard deviation of $X_{i=1\ to\ N}$. The effect of this normalisation is to eliminate the seasonal impact on pressure pattern intensity, thus permitting direct inter-seasonal comparisons.

Once normalised, each field in the extreme wind days data set is compared with all of the other fields in the data set using Pearson product-moment correlations (r_{xy}).

$$r_{xy} = \frac{\sum_{i=1}^{N}\left[\left(x_i - \overline{X}\right)\left(y_i - \overline{Y}\right)\right]}{\sqrt{\sum_{i=1}^{N}\left(x_i - \overline{X}\right)^2 \sum_{i=1}^{N}\left(y_i - \overline{Y}\right)^2}}$$

In this formula, x_i and y_i represent the values at each of the N grid points in the two fields being compared. $\overline{X}$ and $\overline{Y}$ represent the means of the values in the two fields. Pairs of MSLP fields are considered similar if $r_{xy} \geq 0.7$. Yarnal (1993) discusses the numerous sources of subjectivity in choosing a correlation threshold. The value of 0.7 was chosen after experimentation showed that it provided an acceptable balance between the number of patterns produced and the number of days that were not classified.

Once all of the fields have been compared with all of the other fields in the data set, the field with the largest numbers of r_{xy} values meeting the threshold criteria is designated “key pattern” 1 and is considered representative of the first field type. This “key pattern” as well as all the fields with which it is considered to be similar are then removed from the analysis. All fields deemed to

be similar to each of those fields are also removed. The analysis is then repeated with the reduced data set to find “key pattern 2”, and so on, until all fields are classified into m groups of 3 patterns or more. The remainder are considered unclassified.

Once the “key patterns” are established, a second pass over the entire data set is made. This is necessary because it is possible for any particular field to be significantly correlated with more than one pattern. In this step, each field is assigned the “key pattern” with which it is most highly correlated. A second pass was also made over the unclassified fields to assign them to one of the identified “key patterns” A correlation threshold of 0.5 was chosen for this step.

APPENDIX II– CURRENT OBSERVED SWELL AND STORM CHARACTERISTICS FOR WOOLI AND BATEMANS BAY

WOOLI

STORMS (Hs > 3m)

	NE	E	SE	S
Events per year	0.6	3.6	7.9	9.6
Average Hs (m)	3.9	3.5	3.6	3.5
Minimum Hs (m)	3.6	3.0	3.0	3.0
Maximum Hs (m)	4.1	5.4	5.8	5.9
Average Ts (sec)	10.4	9.8	10.2	9.4
Minimum Ts (sec)	10.2	7.4	7.3	7.2
Maximum Ts (sec)	10.6	14.0	13.8	13.6

SWELL WAVES

Percentage Occurrence	Average direction (Degrees from North)	Average Hs (m)	Average Ts (sec)
Waves from dominant direction of incidence (1350 – 1800 clockwise from North)			
48%	157.10	1.7	8.5
Waves from all oceanic directions (100 – 1900 clockwise from North)			
100%	127.20	1.6	8.2

Note: The above values are based on hourly directional wave data obtained at Byron Bay over the period October 1999 to February 2006

BATEMANS BAY:

STORMS (Hs > 3m)

	NE	E	SE	S
Events per year	0.5	2.0	5.7	7.9
Average Hs (m)	3.6	3.3	3.6	3.5
Minimum Hs (m)	3.0	3.0	3.0	3.0
Maximum Hs (m)	4.7	4.4	6.6	5.4
Average Ts (sec)	8.8	10.0	10.1	8.8
Minimum Ts (sec)	7.7	8.0	7.1	6.8
Maximum Ts (sec)	9.6	13.6	15.2	12.0

SWELL WAVES

Percentage Occurrence	Average direction (Degrees from North)	Average Hs (m)	Average Ts (sec)
Waves from dominant direction of incidence (1350 – 1800 clockwise from North)			
54%	154.50	1.4	8.1
Waves from all oceanic directions (100 – 1900 clockwise from North)			
100%	128.80	1.4	7.9

Note: The above values are based on hourly directional wave data obtained at Batemans Bay over the period February 2001 to January 2007